The unique procoagulant adaptations of pseudonaja textilis venom factor V and factor X

Schreuder, M.

Chapter 7

F174-Substituted Human Factor X as Bypassing Agent for Direct Factor Xa Inhibitors

Mark Schreuder, Georges Jourdi, Koen M. Visscher, Ka Lei Cheung, Geraldine Poenou, Daniel Verhoef, Stella Thomassen, Laura F.H. Janssen, Alain Stepanian, Tilman M. Hackeng, Pascale Gaussem, Pieter H. Reitsma, Daan P. Geerke, Virginie Siguret, Mettine H.A. Bos

Manuscript in Preparation

Abstract

Direct factor Xa inhibiting oral anticoagulants are widely used as alternatives to conventional vitamin K antagonists in the management of venous thromboembolism and nonvalvular atrial fibrillation. Unfortunately, bleeding-related adverse effects remain a major safety concern in clinical practice. In case of bleeding or emergency surgery, rapid-onset reversal agents may be required to counteract the anticoagulant activity and restore normal hemostasis. Here we show the ability of F174-substituted human factor X variants to rapidly restore thrombin generation in the presence of direct factor Xa inhibitors (apixaban, rivaroxaban, edoxaban). Their ability to bypass the anticoagulant effects relies on a decreased sensitivity for the direct factor Xa inhibitors due to a disrupted factor Xa-inhibitor binding stability. Furthermore, modification of F174 resulted in a partial loss of inhibition by tissue factor pathway inhibitor, adding to the procoagulant effect of F174-substituted factor X. Consequently, our F174-substituted factor X variant effectively counteracted the anticoagulant effects of apixaban and rivaxoraban in plasma of atrial fibrillation and venous thromboembolism patients. As such, these variants have the potential to serve as a rescue reversal strategy to overcome the effect of direct factor Xa inhibitors in case of life-threatening bleeding events or emergency surgical interventions.

Introduction

Thromboembolic events contribute significantly to morbidity with a global incidence rate of 2.000 cases per 100.000 and have been estimated to account for 1 in 4 deaths, representing the leading cause of mortality worldwide[1]. Individuals with a heightened tendency to form thrombi are at increased risk for ischemic heart disease and stroke, deep-vein thrombosis, pulmonary embolism, and other cardiovascular disorders. The direct oral anticoagulants (DOACs) targeting the key proteases factor Xa (FXa)[2-5] or thrombin[6] are widely used in the management and prevention of thrombotic events[7]. However, major bleeding complications are observed in 1-5% of the patients receiving DOACs[8-10]. Considering that these anticoagulants are prescribed to millions of people worldwide, anticoagulant-associated bleeding will remain a prominent clinical concern[11,12]. Life-threatening or uncontrollable bleeding requires the use of agents that enable rapid reversal of the anticoagulant activity[13,14]. With the direct FXa inhibitors representing the vast majority of DOAC prescription[15,16], access to an effective reversal agent for the direct FXa inhibitors is of critical importance. Currently, andexanet alfa (andexanet)[17], is the only US Food and Drug Administration and European Medicines Agency approved specific reversal agent for the direct FXa inhibitors. While clinical guidelines state that andexanet can be useful for the reversal of rivaroxaban and apixaban, the drug is not readily available at many centers and patient selection is critical[18-21]. In the absence of a specific reversal agent, the guidelines instead recommend administration of 4-factor prothrombin complex concentrate (PCC; 50U/kg) or activated PCC (50U/kg)[18-20].

The development of agents specific for FXa inhibitor reversal is mostly based on recombinant modification of FXa and its inactive zymogen FX[22]. Zymogen FX is composed of a heavy and light chain that are covalently linked via a disulfide bond. The N-terminal light chain consists of a gamma-carboxyglutamic acid (Gla) domain and two epidermal growth factor-like domains that are responsible for anionic phospholipid-binding and have been implicated in macromolecular interactions, respectively[23]. The C-terminal heavy chain comprises an activation peptide that is proteolytically removed upon activation and the serine protease domain that includes the active site, hallmarked by the catalytic triad residues His95, Asp102, and Ser195 (chymotrypsinogen numbering). FX is converted into FXa upon proteolytic activation by the extrinsic factor VIIa (FVIIa) and tissue factor (TF) complex or the intrinsic factor IXa (FIXa) and factor VIIIa (FVIIIa) complex. The newly-formed FXa assembles with its cofactor factor Va (FVa) into the prothrombinase complex that is responsible for the conversion of prothrombin to the active protease thrombin. The spatiotemporal assembly of this complex occurs exclusively on the surface of anionic membranes in the presence of calcium ions.

Downregulation of FXa activity proceeds via inactivation by the endogenous Kunitz-type inhibitor tissue factor pathway inhibitor (TFPI) and serpin antithrombin (AT).

At present, bioengineering of FXa has generated several FXa-based reversal agents that function either by sequestering or bypassing the direct FXa inhibitors. The currently approved antidote andexanet is a catalytically inactive Gla-domainless FXa that functions as a decoy by stoichiometric binding of the inhibitors in order to restore endogenous thrombin generation[24]. Yet, the active site and exosites remain available for potential interactions with pro- and anticoagulant proteins[25-28]. To prevent such macromolecular interactions, Jourdi *et al.* generated a Gla-domainless FXa sequestered by α_2-macroglobulin (GDFXa-α_2M), which retains its affinity for the direct FXa inhibitors[29]. Alternatively, several prohemostatic bypassing agents have been proposed such as a zymogen-like FXa variant (FXa-I16L) exhibiting impaired binding of FXa inhibitors[30,31]. In addition, we recently reported a FX variant comprising an extended 99-loop (FX-C) that sterically prevents interactions with the direct FXa inhibitors[32]. Herein, we showed that the S4 subsite region in the FXa active site, formed by residues Y99, F174, and W215, stabilizes the binding of the FXa inhibitor apixaban. We further demonstrated that disruption of the S4 subsite through alanine-substitution of Y99 and/or F174 resulted in a moderate loss of apixaban sensitivity[32].

In this study, we explored the ability of F174-substituted FX variants to support thrombin generation in the presence of the direct FXa inhibitors. Our data demonstrate that these FX variants exhibit a reduced sensitivity for the natural inhibitor TFPI and for the direct FXa inhibitors due to the destabilization of inhibitor binding. Furthermore, our FX variants were able to restore thrombin generation in plasma derived from atrial fibrillation and venous thrombosis patients treated with apixaban or rivaroxaban. As such, these FX variants have the potential to serve as an alternative therapeutic option to counteract bleeding induced by direct FXa inhibitors.

Material and Methods

Materials: Apixaban (Adooq Bioscience, Irvine, CA, USA) was dissolved to 5 mg/mL in vehicle (10% EtOH, 10% glycerol, 10% PEG400, 3.5% dextrose (v/v)). Rivaroxaban and edoxaban (10 mM in dimethyl sulfoxide (DMSO) were from Hölzel Diagnostika (Cologne, Germany). The peptidyl substrate methoxycarbonylcyclohexylglycylglycyl-Arg-pNA (SpecXa) was from Sekisui Diagnostics (Stamford, CT, USA), and N-α-benzyloxycarbonyl-D-Arg-Gly-Arg-pNA (S2765) and H-D-Phe-Pip-Arg-pNA (S2238) were from Instrumentation Laboratories (Bedford, MA, USA). All tissue culture reagents were from Life Technologies (Carlsbad, CA, USA). Calibrator and fluorescent substrate

(FluCa) were from Thrombinoscope (Maastricht, the Netherlands). FX-depleted human plasma, prothrombin time (PT) reagent (Neoplastine CI Plus), and activated partial thromboplastin time (aPTT) reagent (Triniclot) were from Stago (Asnière-Sur-Seine, France). Normal pooled plasma (NPP) was from Sanquin (Amsterdam, the Netherlands). Unfractionated heparin (UFH) was from LEO Pharma (Ballerup, Denmark). Small unilamellar phospholipid vesicles (PCPS) composed of 75% (wt/wt) hen egg L-phosphatidylcholine (PC) and 25% (wt/wt) porcine brain L-phosphatidylserine (PS) (Avanti Polar Lipids, Alabaster, AL, USA) were prepared and characterized as described[33]. All functional assays were performed in HEPES-buffered saline (HBS: 20 mM HEPES, 0.15 M NaCl, pH 7.5) supplemented with 5 mM $CaCl_2$, 0.1% PEG8000 filtered over an 0.2 µm filter (assay buffer).

Patient Plasma: Blood samples from 89 patients (male/female, 56/44%; mean age, 62 ± 8 years) treated with direct FXa inhibitors were collected from Cochin and Lariboisière University Hospitals (Assistance Publique – Hôpitaux de Paris (AP-HP), Paris, France). Forty-seven patients were treated for non-valvular atrial fibrillation (AF) (23 with apixaban; 24 with rivaroxaban) and 54 for venous thromboembolic (VTE) disease (27 with apixaban; 27 with rivaroxaban). Patients gave their written informed consent, and the investigation was conducted according to the Declaration of Helsinki. Blood was collected in 0.109 M buffered trisodium citrate (9:1 v/v) (Greiner Bio One, Courtaboeuf, France), and platelet-poor plasma (PPP) was prepared following two sequential centrifugation steps at 2500 g for 15 min at room temperature and stored at −80°C. Plasma was briefly thawed at 37°C immediately prior to analysis; all assays were performed in a blinded manner and according to the manufacturers' instructions. Plasma concentrations of direct FXa inhibitors were assessed using a specific anti-Xa assay (STA Liquid Anti-Xa, Stago) on STAR analysers using dedicated calibrators and controls with a lower limit of quantification of 18 ng/mL. Fibrinogen levels were measured by Clauss method (Dade Thrombin, Siemens, Munich, Germany). Prothrombin time results were expressed as international normalized ratio (INR).

Proteins: Human plasma-derived factor V (FV), FVIIa, FIXa, prothrombin, α-thrombin, AT, and the inhibitor dansylarginine-N-(3-ethyl-1,5-pentanediyl)amide (DAPA), RVV-X activator, and corn trypsin inhibitor (CTI) were from Haematologic Technologies (Essex Junction, VT). TFPI) was a generous gift from dr. Cornelis van 't Veer (Amsterdam UMC, The Netherlands). Inhibitory antibodies against the TFPI Kunitz 1 domain, the TFPI Kunitz 2 domain or a mix of anti-Kunitz 1 domain, anti-Kunitz domain 2, and anti-TFPI C-terminus were obtained from Sanquin (Amsterdam, the Netherlands). Human TF (Innovin) was obtained from Siemens (Newark, NY, USA), recombinant factor VIII (FVIII, NovoEight) was from NovoNordisk (Plainsboro, NJ, USA). Recombinant constitutively

active B-domainless human factor V (FV-810; hFV)[34] was large-scale expressed in BHK cells and conditioned media was collected and purified as described[32].

Construction and Purification of Factor X Variants: DNA constructs encoding FX variants comprising the Phe174Ala (FX-F174A), or Phe174Ser (FX-F174S) were prepared from the pCMV4 vector carrying wild-type (wt) human FX[35] by site-directed mutagenesis using the Q5-mutagenesis kit (New England Biolabs; Ipswich, MA, USA). Transfection of the plasmids encoding the FX constructs into HEK293 cells, the selection of stable clones, and the expression and purification of the FX variants were performed as described previously[32]. Partially purified FXa variants were obtained by expanding the stable cell line into three 175 cm^2 cell flasks and conditioning for 24 h in FX-specific expression media. Conditioned media was collected for three consecutive days, centrifuged at 4000 g, filtered over an 0.45 µm polyethersulfone membrane, and supplemented with 1mM benzamidine prior to storage at −20 °C. Following thawing of the conditioned media, the media was ultrafiltrated employing Amicon Ultra-15 centrifugal filter units with 30 kDa molecular weight cutoff to ~2 mL in HBS, 50% (v/v) glycerol, and stored at −20 °C.

Purification of Factor Xa: Purified recombinant FX (r-FX) was activated with RVV-X (1.15 µg/mL FX), applied to a benzamidine sepharose 6B column (GE Healthcare) equilibrated in HBS and eluted using HBS supplemented with 4 mM benzamidine. Fractions were analyzed for FXa activity employing peptidyl substrate hydrolysis (SpecXa). Fractions containing FXa activity were pooled and precipitated using ammonium sulphate (Sigma Aldrich, St Louis, Mo, USA). Precipitate was dissolved to ~3 mg/mL in HBS containing 50% (v/v) glycerol and stored at −20°C. Purified products were visualized by SDS-PAGE employing Coomassie Brilliant Blue staining.

Specific Factor X Activity: The specific extrinsic clotting activity was determined using a modified FX-specific PT-based assay. FX-depleted plasma (45 µL) was mixed with 5 µL FX sample, followed by a 60 s incubation period at 37°C. Coagulation was initiated with the addition of 50 µL PT reagent, and the coagulation time was monitored using a Start4 coagulation instrument (Stago). The specific intrinsic clotting activity was determined using a modified FX-specific aPTT-based assay. FX-depleted plasma (45 µL) was mixed with FX sample (5 µL) and aPTT reagent (50 µL), followed by an 180 s incubation period at 37°C. Coagulation was initiated with the addition of 50 µL of 25 mM CaCl2, upon which the coagulation time was monitored. Reference curves consisted of serial dilutions of NPP. Clotting times were converted to U/mg via the reference curves, assuming 1U FX equals 9 µg/mL.

Macromolecular Substrate Activation: Steady-state initial velocities of macromolecular substrate cleavage were determined discontinuously at 25°C in assay buffer as described[36,37]. Briefly, progress curves of prothrombin activation were obtained by incubating PCPS (50 μM), DAPA (10 μM), and prothrombin (1.4 μM) with recombinant FV-810 (20 nM), and the reaction was initiated with 0.1–0.4 nM of r-FXa, FXa-F174A or FXa-F174S upon which the rate of prothrombin conversion was measured. The kinetic parameters and equilibrium binding constants for prothrombin and cofactor Va (FV-810) were determined using increasing concentration of respective proteins[36]. Prothrombin conversion was assayed in the absence or presence of the direct FXa inhibitors apixaban, rivaroxaban or edoxaban (1 pM–100 μM) in order to determine IC_{50} concentrations for each prothrombinase-assembled FXa variant.

Inhibition by TFPI was assessed using 0-10 nM TFPI incubated with PCPS (50 μM), DAPA (10 μM), prothrombin (1.4 μM) and FV-810 (2 nM). Reactions were initiated with 0.05 nM FXa and at selected time points (5-60 min), aliquots were taken and quenched in HBS supplemented with 50 mM EDTA (EDTA-buffer). The rate of prothrombin conversion was measured as described above and corrected for substrate consumption according to a previously established model system[38]. Inhibitory constant values were determined using normalized thrombin values at 30 min and subsequent analysis by linear regression.

The rate of FX (9.1–2,500nM) activation by the TF-FVIIa complex (TF, 0.1 nM; FVIIa, 0.5 nM) was determined in the presence of PCPS (50 μM) in assay buffer at 25°C. At selected time points (0.5-4 min), aliquots were taken and quenched in EDTA-buffer. The amidolytic activity of each sample was determined by SpecXa conversion (250 μM) and the initial rates of chromogenic substrate hydrolysis were converted to nanomolar of product by reference to a standard curve. The apparent K_M and k_{cat} values for substrate activation were calculated from the Michaelis-Menten equation. For FX activation by the FVIIIa-FIXa complex (FVIIIa 5 nM; FIXa 0.5 nM; PCPS 50 μM) a similar approach was used. FVIII (NovoEight; 40nM) was activated by thrombin (100 nM) for 30 s at 25°C and the reaction was stopped by the addition of a 10-fold molar excess of hirudin. FXa formation was assessed as described above.

Chromogenic Substrate Hydrolysis. The kinetics of peptidyl substrate hydrolysis were measured in assay buffer using increasing concentrations of SpecXa (10–600 μM) or S2765 (1.2–1200 μM) and initiated with 5 nM of the FXa variants. Chromogenic conversion was assayed in the absence or presence of the direct FXa inhibitors apixaban, rivaroxaban or edoxaban (0.0001–100 μM; SpecXa 250 μM) in order to determine IC_{50} concentrations for each free FXa variant.

Inhibition of Factor Xa by Antithrombin. The rate of inactivation of FXa by AT was measured in assay buffer under pseudo-first-order rate conditions at ambient temperatures. Uncatalyzed reactions were prepared in assay buffer containing 0.1–0.8 µM AT and 7.5 nM FXa. At 0–110 min residual enzyme activity was determined with the addition of 250 µM SpecXa. Catalyzed reactions were prepared in assay buffer containing 0.5–6 mIE/mL UFH, 0.5 µM AT, initiated with 5nM FXa. At 0.5–10 min residual enzyme activity was determined with the addition of 250 µM SpecXa. The rate of AT inhibition was determined by fitting the obtained values to an exponential decay function (*k*1) and subsequent analysis by linear regression (*k*2) using GraphPad Prism software suite.

Calibrated Automated Thrombography. Thrombin generation curves were obtained by supplementing NPP with TF (2 or 6 pM), CTI (70 µg/mL), PCPS (20 µM), and 15–45 µg/mL FX variant in the absence or presence of the direct FXa inhibitors apixaban, rivaroxaban or edoxaban. Thrombin formation was initiated by addition of substrate buffer (FluCa) to the plasma. The final reaction volume was 120 µL, of which 80 µL was plasma. Thrombin formation was determined every 15 s for 30–60 min and corrected for the calibrator using Thrombinoscope software. The lag time, mean endogenous thrombin potential (ETP), thrombin peak height, and velocity index were calculated from at least three individual experiments.

Molecular Dynamics Simulations. Molecular Dynamics (MD) simulations of FXa-F174A and FXa-F174S in complex with apixaban were performed using GROMACS version 5.1.4[39], starting from the crystal structure with PDB ID 2P16[5] in which F174 was mutated *in silico* into alanine or serine, respectively. Starting from these structures, energy minimization and four independent MD simulations were performed per system (starting from different randomly assigned atomic velocities), using identical set-up and settings as previously described for FXa simulations[32]. Each production MD run as used for further analysis was 500 ns long, and root-mean-square deviations (RMSDs) during simulation of apixaban atomic positions were calculated after conformational fitting on the MD starting structure with respect to backbone atoms of the protein. Averaging over 10 ns intervals generated block-averaged time series for the analyzed data, and subsequently standard deviations were computed.

Statistical Analysis: All statistical analyses were computed using the GraphPad Prizm software. Kinetic data were analyzed by nonlinear regression using a three-parameter logistic function. Coefficients of determination (R^2) were given by linear regression. Parameters of calibrated automated thrombography in patient plasma and in the absence versus presence of TFPI-inhibiting antibodies were compared by one-way

ANOVA. Statistical significance was accepted for p-value of <0.05. All data are presented as mean ± 1 standard deviation and are the result of at least two-three experiments, unless stated otherwise.

Results

Characterization of F174-substituted Factor X Variants. Previously we reported that partially purified F174A-substituted FXa demonstrates a moderate loss of sensitivity for the direct FXa inhibitor apixaban (9-fold enhanced IC_{50}) while retaining procoagulant activity[32]. In addition to an alanine replacement, the S4 subsite Phe174 was also substituted by a similarly hydrophobic Ile residue and a hydrophilic Ser, thereby generating FX-F174I and FX-F174S, respectively. Following stable FX expression in HEK293 cells, initial analysis of partially purified FXa variants revealed a reduced apixaban inhibition (10-16-fold enhanced IC_{50}) (**Figure S1**), consistent with earlier observations[32]. Given that all F174-substituted variants displayed similar IC_{50} values for apixaban inhibition, we next subjected the FX variants with the most significant change in the S4 subsite (FX-F174A and FX-F174S) to further characterization following purification. SDS-PAGE analysis showed each FX(a) variant to migrate similar to recombinant wild-type FXa (r-FXa) **(Figures 1A,B; S2)**. Analysis of PT- or APTT-based fibrin clot formation initiated by the extrinsic **(Figure 1C)** or intrinsic coagulation pathway **(Figure 1D)** revealed FX-specific clotting activities similar to that of r-FX**,** indicating that substitution of F174 by either alanine or serine does not affect FXa procoagulant function.

F174 Substitution in Factor X Reduces the Sensitivity for the Direct Factor Xa Inhibitors. In concordance with a reduced apixaban inhibition in partially purified FXa variants **(Figure S1)**, assessing the inhibitory constant of the direct FXa inhibitors in a purified system demonstrated a ~2-5-fold reduced sensitivity for purified free FXa-F174 variants relative to r-FXa. Assembly of FXa-F174 variants into prothrombinase resulted in a 5-10-fold decreased sensitivity for inhibition by either apixaban, rivaroxaban or edoxaban compared to r-FXa **(Table 1)**. These results confirm our initial observations and suggest that F174-substituted FXa variants might support thrombin generation in the presence of the direct FXa inhibitors.

To determine the capacity of the purified F174-substituted FX variants to overcome inhibition by the direct FXa inhibitors, their thrombin-forming potential was assessed using a high TF-trigger (6 pM) resulting in direct FX activation by TF-FVIIa. Following supplementation of NPP with r-FX at three-fold the FX plasma concentration (30 µg/mL), apixaban dose-dependently decreased thrombin peak with half-maximum inhibition

at 0.1μM **(Figure 2A; Table S1).** The latter was markedly higher than the values of free FXa inhibition in a purified system **(Table 2)**[5], which may be due to the plasma setting and supraphysiologic amounts of FX in this system. Conversely, supplementation with FX-F174A or FX-F174S resulted in a 15-35-fold reduction in apixaban sensitivity relative to r-FX **(Figure 2A; Table S1)**. In a similar fashion, addition of F174-substituted FX variants demonstrated a 10-15-fold reduced sensitivity to inhibition by rivaroxaban or edoxaban compared with r-FX **(Figure 2B,C; Table S1)**. Next, the ability of the FX variants to support thrombin generation was explored under conditions when FX activation is mainly driven by FIXa[40,41], via the so-called Josso loop using a low amount of TF (2 pM). Similar to previous observations, supplementation with either FX-F174A or FX-F174S demonstrated a 10-40-fold reduced sensitivity for apixaban, rivaroxaban, or edoxaban relative to r-FX **(Figure S3; Table S1)**.

S4 Subsite Displacement of Apixaban in Complex with F174-substituted Factor Xa. To gain insight into the molecular mechanism underpinning the reduced sensitivity of the F174-substituted FXa variants for the FXa inhibitors, we performed MD simulations of the FXa variants in complex with apixaban. The F174A and F174S substitutions were modelled into apixaban-bound FXa (PDB ID 2P16)[5], and four 500 ns MD simulations of each FXa–apixaban complex were independently performed. Each simulation was initiated from an identical conformation but with different atomic starting velocities. As we previously described[32], MD simulations with wild-type FXa produced little if any shifts in apixaban positioning, which is indicative of a high binding stability of apixaban in the FXa active site **(Figure 3A)**. In contrast, substantial movement of the apixaban molecule was observed in the MD trajectories of at least two out of the four simulations of the FXa-F174A and FXa-F174S apixaban complexes **(Figure 3B,C)**. This was reflected by root-mean-square deviation (RMSD) values of >0.1 nm, as well as by displacement of apixaban from either the S4 subsite alone or in combination with displacement from the S1 subsite. As such, these findings indicate an enhanced mobility of apixaban in the FXa active site and a loss of apixaban binding stability following F174-substitution.

Reduced TFPI Inhibition of F174-substituted Factor Xa Augments the Direct Factor Xa Inhibitor Bypassing Effect. We next assessed the kinetic parameters of the FXa-F174 variants to examine the effects of F174 substitution on the FXa active site. Evaluation of the ability of the FXa variants to hydrolyze the FXa-specific chromogenic substrates SpecXa and S2765 revealed no differences in k_{cat} relative to r-FXa **(Table 2)**. Conversely, the binding affinities of both substrates were significantly altered in the FXa-F174 variants **(Table 2)**, indicative of a modified substrate binding cleft. This would imply that either the chromogenic substrates engage the FXa S4 subsite[42] or that F174 substitution induces conformational changes in the substrate binding

region. Importantly, the kinetic parameters of prothrombin conversion by the FXa-F174 variants, as well as the apparent binding affinity for the FVa-like cofactor FV-810, were similar to those of r-FXa **(Table 2)**. This demonstrates that F174 modification does not significantly impact the assembly of the prothrombinase complex or the catalytic efficiency of FXa's natural substrate prothrombin.

To examine the effects of F174 substitution on FXa inhibition, we assessed the second-order rate constants of the natural active site inhibitor AT. Inhibition of FXa-F174 variants proceeded at an identical rate relative to r-FXa in the absence or presence of UFH **(Table 1**), consistent with previous reports[32,43,44]. These observations might reflect the interaction of AT with the FXa S1 subsite rather than the S4 subsite, as shown by X-ray structures[45,46]. On the other hand, assessment of prothrombinase-assembled FXa inhibition by the natural active site inhibitor TFPI revealed that FXa-F174A and FXa-F174S displayed a 1.3- and 4.5-fold reduced TFPI sensitivity relative to r-FXa, respectively **(Figure 4, Table 1)**. To gain more insight in the TFPI resistance, we next explored the thrombin-forming potential of FX-F174 variants using calibrated automated thrombography in plasma supplemented with antibodies that specifically block the function of individual TFPI domains. In the absence of TFPI antibodies, FX-F174 variants displayed a two-fold increased thrombin peak height relative to r-FX **(Figure S4)**. In contrast, similar thrombin peak heights were observed in the presence of TFPI-inhibiting antibodies **(Figure S4)**. This indicates that the initial increased thrombin-forming potential of FX-F174 variants is induced by a partial loss of inhibition by TFPI. As such, these results suggest an additional mode of action by which the F174-substituted FX variants bypass the direct FXa inhibitors.

F174-substituted Factor X Variants Bypass the Direct FXa Inhibitors and Restore Thrombin Generation. The reduced sensitivity for the direct FXa inhibitors and TFPI **(Table 1, S1)** might enable FX-F174 variants to reverse the anticoagulant effect of the direct FXa inhibitors. We therefore studied the ability of our FX-F174 variants to overcome therapeutic peak inhibitor levels[47-49] using calibrated automated thrombography in response to a high TF-trigger (6 pM). Following supplementation of NPP with apixaban, rivaroxaban, or edoxaban (1 μM), r-FX (60 μg/mL) only minimally improved the thrombin generation (up to 20% of NPP peak height; **Figure 5A**). In contrast, supplementation with 30 μg/mL FX-F174A or FX-F174S fully restored the thrombin generation in the presence of apixaban, whereas 15 μg/mL improved the thrombin peak height to 75% of NPP **(Figure 5B)**. Similarly, the anticoagulant activity of rivaroxaban was completely reversed by the FX-F174 variants **(Figure 5C)** and improved up to 60-75% of NPP in edoxaban-spiked plasma **(Figure 5D)**. This is consistent with the initially observed ~11-fold increase in IC_{50} for edoxaban compared to the 15-35-fold increase for apixaban or

rivaroxaban **(Table S1)**. Of note, supplementation with the FX-F174 variants prolonged both the lag time and time to peak by 1.3-2-fold in the presence but not in the absence of an inhibitor **(Figure S5)**. However, this delay in thrombin generation was not induced by a diminished FX activation considering the steady-state kinetics for activation by the intrinsic or extrinsic tenase complexes were unperturbed **(Table S2)**. Furthermore, no delay in the activation of FV was observed since FXa-F174A activated FV in an identical manner to r-FXa **(Figure S6)**. In addition, assessment of the thrombin-forming potential under conditions of a limited TF-trigger (2 pM) revealed that the anticoagulant activity of the direct FXa inhibitors was largely reversed via supplementation of 15-30 µg/mL FX-F174A or FX-F174S **(Figure S7)**. Consistent with previous results in the presence of a high TF-trigger, the FX-F174 variants maintained an increased lag time relative to NPP in the absence of an inhibitor.

F174-substituted Factor X Reverses the Anticoagulant Activity of Apixaban and Rivaroxaban in Atrial Fibrillation and Venous Thromboembolism Patient Plasma. Since both FX-F174 variants behaved in a similar fashion, we selected FX-F174A for assessment in patient plasma. The ability of FX-F174A to bypass the direct FXa inhibitors was validated in plasma derived from AF and VTE patients who were treated with apixaban or rivaroxaban **(Table S3)** using calibrated automated thrombography in response to a high TF-trigger (6 pM). Assessment of the thrombin-forming potential demonstrated that supplementation of patient plasma with FX-F174A increased the thrombin peak height in all individual patient samples **(Figure 6A,B)**. In AF patient plasma, the thrombin peak height was increased to near-NPP conditions (290-330 nM). In addition to the thrombin peak height, AF and VTE patient plasma displayed a significant prolonged lag time relative to NPP **(Figure 6C)**. Supplementation with FX-F174A markedly shortened the lag time in all individual patients samples **(Figures 6C,D)**. Additional assessment revealed that FX-F174A reversed the anticoagulant effect on the thrombin generation velocity in similar fashion as the thrombin peak height and lag time **(Figures S8A,B)**. In contrast, the ETP in AF and VTE patient plasma was only modestly reduced in the absence of FX-F174A relative to NPP **(Figures S8C,D)** as a result of the inhibitor-induced extension of the thrombin generation curves over time. Still, FX-F174A significantly elevated the ETP in all patient groups. As such, these results demonstrate that F174-substituted FX variants have the ability to reverse the anticoagulant activity of the direct FXa inhibitors in patient plasma.

Discussion

In this study, we present FX variants that could act as prohemostatic bypassing agents by initiating coagulation in the presence of direct FXa inhibitors. We showed that a FX variant comprising a single substitution in the S4 subsite effectively counteracted the anticoagulant effects of apixaban or rivaroxaban in plasma from AF and VTE patients. While FX-F174A is inhibited by rivaroxaban and apixaban to some extent (**Figure S9**), FX-F174A is nonetheless capable of promoting thrombin formation in the presence of therapeutic concentrations of FXa inhibitor. Unfortunately, we were unable to obtain plasma samples from the same individual patients before treatment initiation. As thrombin generation profiles of individual plasmas can vary substantially, such samples would provide valuable information on the level of anticoagulant reversal in these patients [50]. Nevertheless, our FX variant successfully restored the thrombin-forming potential within the therapeutically useful inhibitor range (>100 nM), at which patients are likely at an increased risk for bleeding[49].

In the presence of therapeutic peak inhibitor levels we were able to restore thrombin generation using 15-45 µg/mL of our F174-substituted FX variants. The increased amounts of FX-F174 variant that are required to bypass the direct FXa inhibitors relative to the FX plasma concentration[51] could reflect the competition for activation by the intrinsic and extrinsic tenase complexes with endogenous FX. Furthermore, FX-F174 variants displayed a 1.3-2-fold increase in lag time compared to r-FX. However, the kinetic constants for the activation of FX by the intrinsic or extrinsic tenase complexes were unperturbed. Moreover, a delay in the FXa-mediated activation of FV is known to specifically prolong the thrombin generation lag time[52], yet the activation of FV was identical between FXa-F174A and r-FXa. An alternative explanation might be a delay in FV activation in the presence of the direct FXa inhibitors. The small amounts of FXa that are being generated during the initial phase of coagulation are likely targeted by direct FXa inhibitors. Minor differences in the affinity of these inhibitors for FXa might therefore induce the observed inhibitor-dependent prolongation in lag time.

Interestingly, we observed a reduced sensitivity of FXa-F174 variants for the natural inhibitor TFPI. Previous studies have shown that the inhibition or sequestration of TFPI could restore hemostasis in hemophilic plasma and patients[25,26,53-55], thus providing evidence for an additional mode of action by which our FX-F174 variants are able to bypass direct FXa inhibitors. Despite the three-fold reduction in TFPI sensitivity of FXa-F174S relative to FXa-F174A **(Figures 4,S4, Table 2)**, their minor functional differences might be explained by the relatively low plasma concentration of free TFPIα (~0.3nM)[56,57]. The partial resistance for TFPI might also explain the augmented IC_{50} values of FX-F174

variants for the direct FXa inhibitors observed in plasma relative to the inhibition of free or prothrombinase-assembled FXa. Collectively, our findings reveal that FX-F174 variants bypass direct FXa inhibitors via an unique mechanism compared to previously described reversal agents and indicate that modulation of FXa inhibition by TFPI might be a viable strategy to overcome the anticoagulant effects of direct FXa inhibitors.

To get further insights into the mechanistic principles of our FX-F174 variants, we examined the impaired FXa-apixaban interaction using MD simulations. Although the active site of FXa is able to accommodate the inhibitor, the increased mobility of apixaban following F174 substitution indicates a loss of binding stability. Previous studies suggested an important role for the S4 subsite in the stabilization of apixaban binding[5,32]. In line with our MD simulations the S4 subsite is confirmed to be less compact due to the substitution of the large aromatic phenylalanine by the relatively small alanine or serine **(Figure S10)**, resulting in decreased binding stability. Interestingly, Qu *et al.* recently performed similar MD simulations (with lengths of 200-500 ns) using a modelled FXa-F174A variant based on the FXa-rivaroxaban X-ray structure[58]. In contrast to our results using apixaban, the slightly smaller and more flexible rivaroxaban ligand was completely released into the solvent within 100 ns in three out of five simulations. In the two other trajectories, the P_4 moiety of rivaroxaban shifted into the S1′ pocket between residues F41, Q61, and Q192. These differential effects suggest that the binding stability of rivaroxaban is even more impacted upon F174 substitution compared to apixaban. Substitution of F174 for alanine or serine induces minor conformational modifications in the FXa active site, as shown by the reduced catalytic activity towards FXa-specific chromogenic substrates. However, plasma clotting and kinetic assays demonstrated that the conversion of the natural substrate prothrombin remained unaltered, suggesting that prothrombin does not engage in productive interactions with the S4 subsite of FXa. Alternatively, these results might suggest that exosites in FXa and prothrombin drive the proteolytic cleavage at the prothrombin activation residues R271 and R320[59,60]. Although our data does not provide any indication, it should be noted that the FXa-F174 variants might have potential off-target interactions that have not been uncovered by the *in vitro* experimental systems.

A limitation of our approach may be the use of a recombinant protein variant that could elicit an immunogenic response, thereby limiting the efficacy of repeated use. Since our FX variants comprise a single amino acid substitution, the risk for immunogenicity might be minimal. Thus far, neutralizing antibody responses against andexanet alfa have not been reported and neither have antibodies with cross-reactivity to factor X(a) been detected[17,61]. Non-neutralizing antibodies have been developed albeit with generally low antibody titers[61]. Importantly, only a few cases of patients with acquired inhibitors

against FX have been reported[62], suggesting that either FX or its derived variants have little immunogenic potential. It is also important to note that prohemostatic bypassing agents may significantly increase the risk for thrombotic complications and therefore require intensive evaluation in clinical practice. For safety purposes, we employed F174-substituted FX variants in an inactive zymogen form, which would prevent potential macromolecular interactions. Upon the initiation of secondary hemostasis, FX-F174 variants are activated through the intrinsic and extrinsic pathways in a similar manner as endogenous FX. As such, major disturbances that could fail to stop bleeding or otherwise induce pathological thrombosis might be prevented.

In conclusion, our findings show that via a single residue substitution we have created a FX variant that exhibits a decreased sensitivity for direct FXa inhibitors and is partially resistant to inhibition by TFPI. We further demonstrated the ability of F174-substituted FX variants to reverse the anticoagulant activity of apixaban and rivaroxaban in plasma of AF and VTE patients. As such, these variants have the potential to serve as a rapid-onset prohemostatic bypassing strategy to counteract life-threatening bleeding complications as a result of direct FXa inhibitors.

Acknowledgements

This work was financially supported by the Bayer Hemophilia Awards Program (Special Project Award) and Landsteiner Foundation for Blood Transfusion (LSBR, grant. no. 1451). The funding agencies had no role in the preparation, review, or approval of the manuscript.

Figures

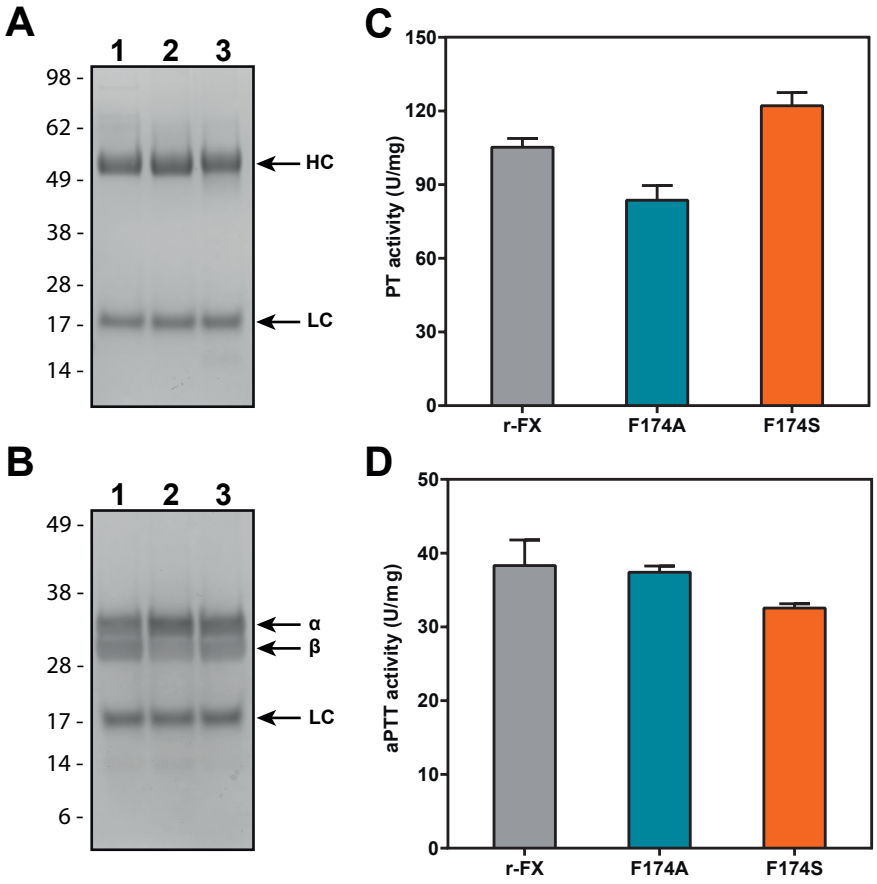

Figure 1. Characterization of F174-substituted factor X(a) variants. (A-B) SDS-PAGE analysis of purified recombinant FX **(A)** or FXa **(B)** variants (2 µg/lane) under reducing conditions and visualized by staining with Coomassie Brilliant Blue R-250. Lane 1, wild-type FX(a); lane 2, FX(a)-F174A; lane 3, FX(a)-F174S. The protein bands corresponding to the FX heavy chain (HC), the heavy chain derived from α or β FXa (α or β), the FX(a) light chain (LC), and the apparent molecular weights (kDa) of the standards are indicated. The purified FXa products migrate as a mixture of α and β FXa, with the latter resulting from autoproteolytic excision of the C-terminal portion of FXa-α (residues 436–447). Both α and β FXa isoforms are functionally similar with respect to prothrombinase assembly, prothrombin activation, antithrombin recognition, and peptidyl substrate conversion[63]. **(C-D)** The specific clotting activity of wild-type FX (r-FX), FX-F174A (F174A), or FX-F174S (F174S) initiated by the extrinsic **(C)** or intrinsic **(D)** pathway using a prothrombin time (PT)-based or activated partial thromboplastin time (aPTT)-based assay as described in 'Materials and Methods'. Mean values are given ± 1 S.D. Data are representative of three independent experiments.

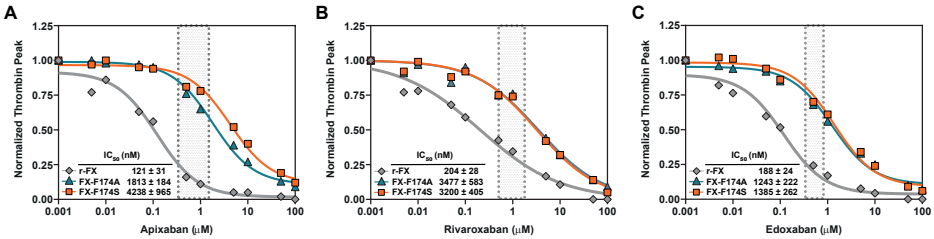

Figure 2. F174-substituted factor X variants facilitate thrombin generation in the presence of the direct factor Xa inhibitors. Thrombin generation was measured for 60 min at 37°C in normal pooled plasma supplemented with 30 µg/mL of r-FX (*grey diamonds*), FX-F174A (*blue triangles),* or FX-F174S (*orange squares*) and increasing concentrations (1 nM-100 µM) of apixaban **(A)**, rivaroxaban **(B),** or edoxaban **(C)**. Thrombin formation was triggered by the addition of 6 pM TF in the presence of 20 µM PCPS and initiated with $CaCl_2$ and a thrombin fluorogenic substrate as detailed in 'Materials and Methods'. The thrombin peak height was normalized to the peak height in the absence of inhibitor, and the lines were drawn by fitting the data to a three-parameter logistic function upon which the IC_{50} ± 1 standard deviation of the induced fit were obtained (**Table S1**), which are shown in the insert. The grey dotted areas represent therapeutic peak inhibitor levels (apixaban, 0.35-1.5 µM; rivaroxaban, 0.5-2 µM; edoxaban, 0.25-0.9 µM). Data are representative of three independent experiments.

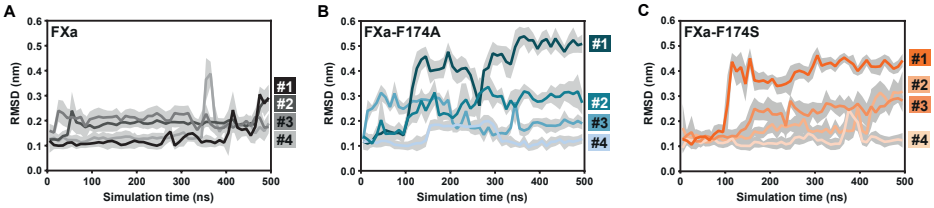

Figure 3. Molecular Dynamics of apixaban bound to factor Xa variants. MD simulations were performed using the X-ray structure of apixaban-bound factor Xa (PDB ID: 2P16)[5]. **(A, data from reference[32])**. Substitutions of phenylalanine 174 were modelled in order to generate FXa-F174A **(B)** or FXa-F174S **(C)** and were used here for respective simulations. Root-mean-square deviations (RMSDs, with respect to 2P16) of atomic positions of the apixaban ligand during four independent 500 ns simulations are presented as block averages over 10 ns intervals (#1-#4). The corresponding single standard deviation intervals are indicated (*gray density*).

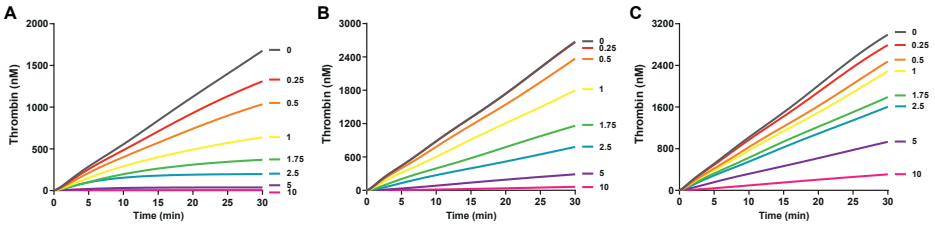

Figure 4. Inhibition of factor Xa variants by tissue factor pathway inhibitor (TFPI). The inhibition of factor Xa by TFPI was assessed by measuring the prothrombinase-dependent conversion of prothrombin. Reaction mixtures containing 1.4 μM prothrombin, 2 nM FV-810, 50 μM PCPS, 10 μM DAPA were initiated with 0.05 nM r-FXa **(A)**, FXa-F174A **(B)**, or FXa-F174S **(C)** in the presence of 0-10 nM TFPI. At selected time intervals, samples were removed and thrombin formation was assessed by S2238 (250 μM) conversion. The data was corrected for substrate consumption as described in 'Materials and Methods'. The data sets are representatives of two independent experiments.

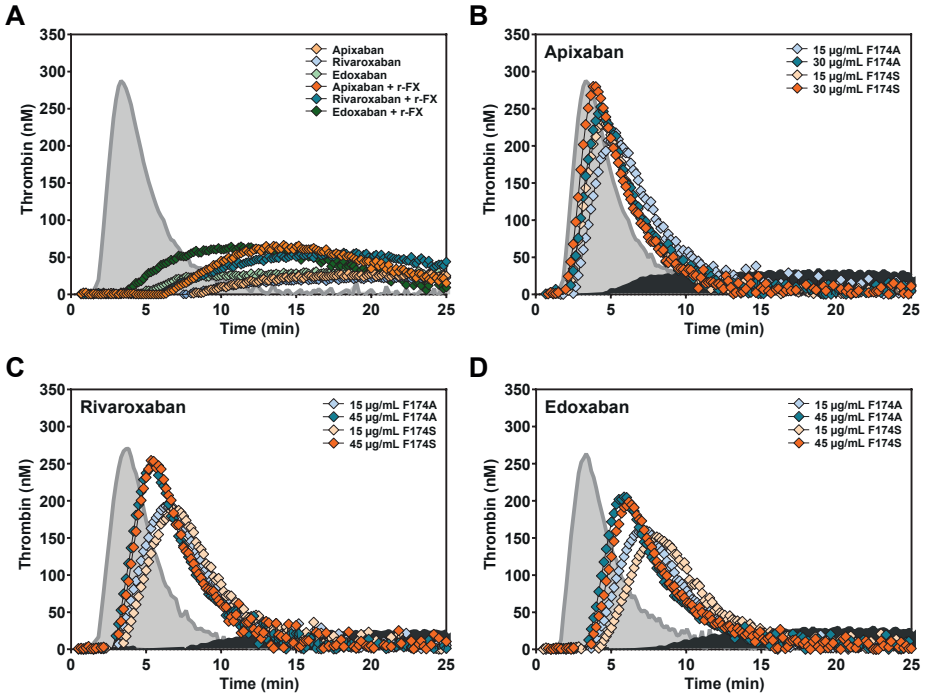

Figure 5. F174-substituted factor X variants restore thrombin generation in inhibitor-spiked plasma. Thrombin generation was measured for 60 min at 37°C in normal pooled plasma (NPP) supplemented with **(A)** 1 µM apixaban, rivaroxaban, or edoxaban in the absence (*yellow, light blue, or light green diamonds, respectively*) or with addition of 60 µg/mL r-FX (orange, dark blue or dark green, respectively), **(B)** 15-30 µg/mL FX-F174A (*light blue-dark blue diamonds*) or FX-F174S (*yellow-orange diamonds*) and apixaban (1 µM), or **(C-D)** 15-45 µg/mL FX-F174A (*light blue-dark blue diamonds*) or FX-F174S (*yellow-orange diamonds*) and 1 µM rivaroxaban **(C)** or edoxaban **(D)**. Thrombin formation was triggered by the addition of 6 pM TF in the presence of 20 µM PCPS and initiated with $CaCl_2$ and a thrombin fluorogenic substrate as detailed in 'Materials and Methods'. The thrombin generation curves of NPP in the absence **(A-D)** (light gray area under the curve) or presence **(B-D)** (dark gray area under the curve) of the inhibitors are shown. Data sets are representatives of three independent experiments.

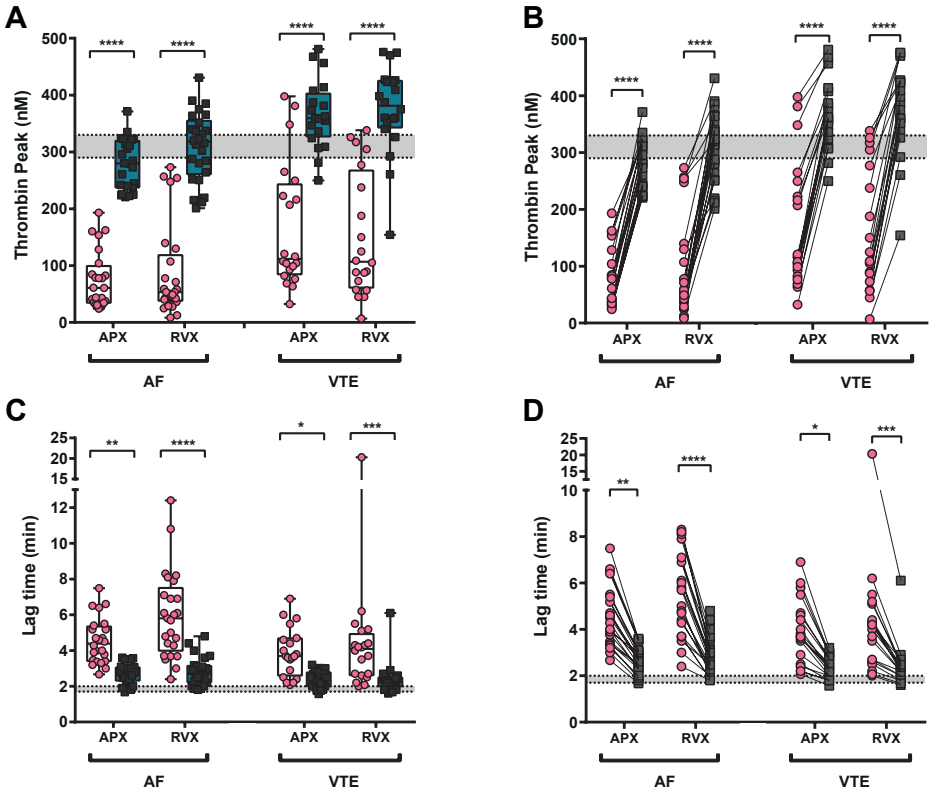

Figure 6. Reversal of the anticoagulant activity of apixaban or rivaroxaban in atrial fibrillation and venous thromboembolism patient plasma. Thrombin generation was measured for 60 min at 37°C in plasma from atrial fibrillation (AF) or venous thromboembolism (VTE) patients treated with apixaban (APX) or rivaroxaban (RVX) in the absence (*pink dots*) or supplemented (*grey squares*) with 30 µg/mL FX-F174A. Thrombin formation was triggered by the addition of 6 pM TF in the presence of 20 µM PCPS and initiated with CaCl2 and a thrombin fluorogenic substrate as detailed in 'Materials and Methods'. The thrombin peak height **(A-B)** and lag time **(C-D)** are shown. The thrombin peak height and lag time of individual patient plasma in the absence or supplemented with FX-F174A are shown by connected lines **(B, D)**. Bars represent the mean, grey dotted areas represent NPP values (n=13; thrombin peak, 290-330 nM; lag time, 1.7-2 min). *p<0.05, **p<0.01, ***p<0.001, ****p<0.0001 according one-way ANOVA. Each data point represents a single measurement performed for each patient sample.

	Apixaban[a] IC_{50} (nM)	Rivaroxaban[a] IC_{50} (nM)	Edoxaban[a] IC_{50} (nM)	Apixaban[b] IC_{50} (nM)	Rivaroxaban[b] IC_{50} (nM)	Edoxaban[b] IC_{50} (nM)	Antithrombin[a] $k2$, uncatalyzed (M^{-1} S^{-1} x 10^3)	Antithrombin[a] $k2$, UFH (M^{-1} S^{-1} x 10^6)	TFPI[b] K_i (nM)
r-FXa	5.9 ± 0.3	2.5 ± 0.1	7.9 ± 0.2	9.2 ± 1.0	1.6 ± 0.2	5.3 ± 0.6	5.3 ± 0.1	2.0 ± 0.2	0.8 ± 0.04
FXa-F174A	24.6 ± 1.5	9.6 ± 0.3	16.5 ± 0.4	57.5 ± 7.4	12.1 ± 1.9	40.6 ± 4.3	4.7 ± 0.5	2.6 ± 0.1	1.3 ± 0.25
FXa-F174S	20.9 ± 1.1	14.3 ± 0.2	28.5 ± 0.4	55.6 ± 5.4	16.2 ± 1.7	24.2 ± 2.6	5.0 ± 0.5	3.8 ± 0.2	3.3 ± 0.48

Table 1. Kinetic constants for inhibition of free or prothrombinase-assembled factor Xa. The kinetic constants for free[a] or prothrombinase-assembled[b] factor Xa were obtained as described in 'Materials and Methods'. Fitted values ± 1 standard deviation of the induced fit are the means of two to three independent experiments.

	SpecXa[1] K_m (μM)	SpecXa[1] k_{cat} (min^{-1})	S2765[1] K_m (μM)	S2765[1] k_{cat} (min^{-1})	Prothrombin[2] K_m (μM)	Prothrombin[2] k_{cat} (min^{-1})	Cofactor Va[2] $K_{d,\ app}$ (nM)
r-FXa	113 ± 9	23.9 ± 0.6	85 ± 10	34.3 ± 1.1	0.52 ± 0.10	960 ± 83	0.8 ± 0.2
FXa-F174A	251 ± 7	25.8 ± 0.3	360 ± 33	32.6 ± 1.2	0.70 ± 0.23	1041 ± 163	1.2 ± 0.1
FXa-F174S	186 ± 9	30.6 ± 0.6	217 ± 17	21.9 ± 0.6	0.69 ± 0.08	1152 ± 73	0.9 ± 0.2

Table 2. Kinetic parameters for peptidyl substrate and macromolecular conversion. The kinetic constants for free[(1)] or prothrombinase-assembled[(2)] factor Xa were obtained as described in 'Materials and Methods'. Fitted values ± 1 standard deviation of the induced fit are the means of two to three independent experiments.

Supplementary Figures and Tables

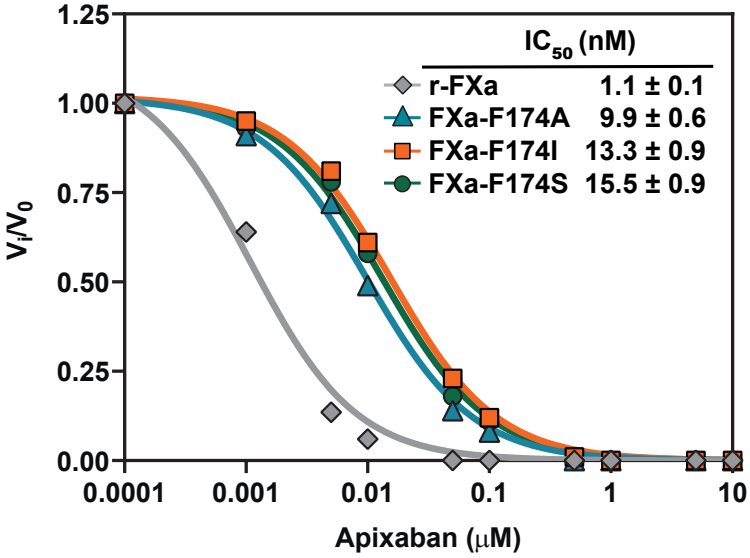

Supplementary figure 1. Apixaban inhibition of partially purified factor Xa variants. The rate of peptidyl substrate conversion (250 μM SpecXa) by 5 nM of RVV-X-activated r-FX (*grey diamonds*), FX-F174A (*blue triangles*), FX-F174I (*green circles*), or FX-F174S (*orange squares*) was determined in the absence (V_0) or presence (V_i) of increasing apixaban concentrations (0.1 nM–10 μM). The lines were drawn by fitting the data to a three-parameter logistic function, and the fitted parameters for IC_{50} ± 1 standard deviation of the induced fit are shown in the inset. Data are the means of two independent experiments.

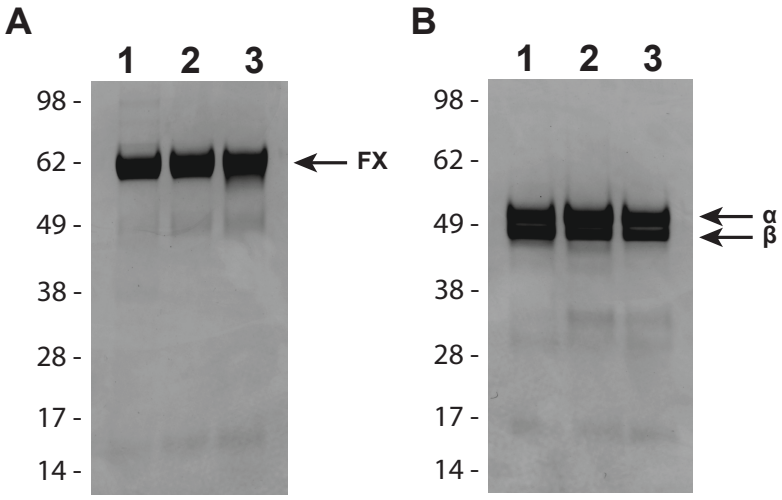

Supplementary figure 2. SDS-PAGE analysis of F174-substituted factor X(a) variants. SDS-PAGE analysis of purified recombinant FX **(A)** or FXa **(B)** variants (2 µg/lane) under non-reducing conditions and visualized by staining with Coomassie Brilliant Blue R-250. Lane 1, wild-type FX(a); lane 2, FX(a)-F174A; lane 3, FX(a)-F174S. The protein bands corresponding to full-length FX (FX), the full length α or β FXa (α or β), and the apparent molecular weights (kDa) of the standards are indicated. The purified FXa products migrate as a mixture of α and β FXa, with the latter resulting from autoproteolytic excision of the C-terminal portion of FXa-α (residues 436–447). Both α and β FXa isoforms are functionally similar with respect to prothrombinase assembly, prothrombin activation, antithrombin recognition, and peptidyl substrate conversion[63].

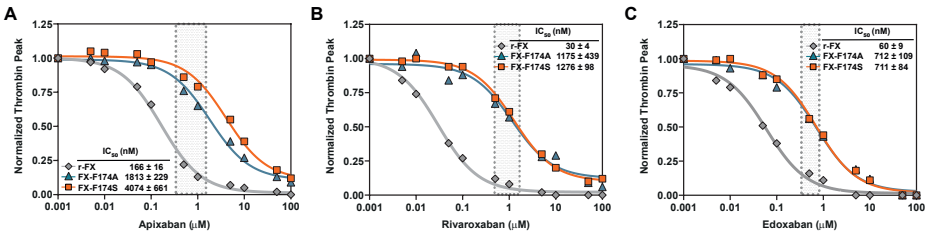

Supplementary figure 3. F174-substituted factor X variants facilitate thrombin generation in the presence of the direct factor Xa inhibitors following a low TF-trigger. (A-C) Thrombin generation was measured for 60 min at 37°C in normal pooled plasma supplemented with 30 µg/mL of r-FX (*grey diamonds*), FX-F174A (*blue triangles)* or FX-F174S (*orange squares*) and increasing concentrations (0.001-100 µM) of apixaban **(B)**, rivaroxaban **(C)** or edoxaban **(D)**. Thrombin formation was triggered by the addition of 2 pM TF in the presence of 20 µM PCPS and initiated with $CaCl_2$ and a thrombin fluorogenic substrate as detailed in 'Materials and Methods'. The thrombin peak height was normalized to the peak height in the absence of inhibitor, and the lines were drawn by fitting the data to a three-parameter logistic function upon which the IC_{50} ± 1 standard deviation of the induced fit were obtained (**Table S1**), which are shown in the insert. The grey dotted areas represent therapeutic peak inhibitor levels (apixaban, 0.35-1.5 µM; rivaroxaban, 0.5-2 µM; edoxaban, 0.25-0.9 µM). Data are representative of three independent experiments.

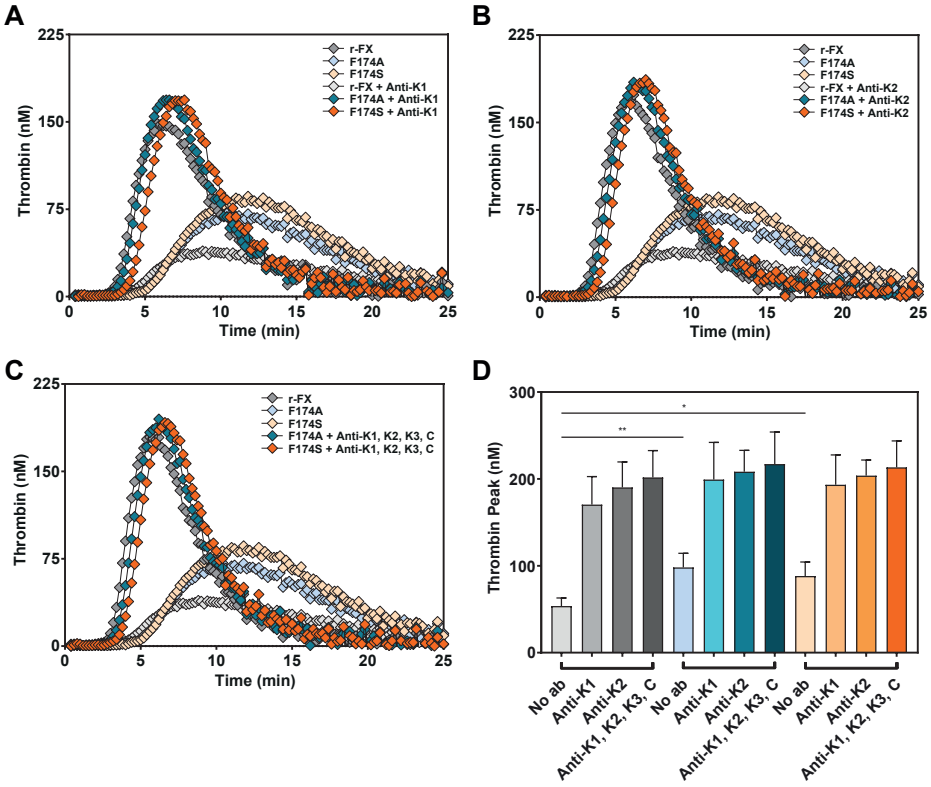

Supplementary figure 4. Blocking of tissue factor pathway inhibitor (TFPI) during thrombin generation by F174-substituted factor X variants. Thrombin generation was measured for 60 min at 37°C in FX-depleted plasma supplemented with 10 µg/mL r-FX, FX-F174A, or FX-F174S in the absence (*white, light blue,* and *yellow diamonds, respectively*) or presence (*grey, dark blue, and orange diamonds, respectively*) of TFPI blocking antibodies against the Kunitz 1 domain **(A,** 10 µg/mL**)**, the Kunitz 2 domain **(B,** 50 µg/mL**),** or the Kunitz 1 domain, Kunitz 2 domain, and C-terminus **(C,** 50 µg/mL**)**. **(D)** Thrombin peak height was plotted for each condition and the results are presented as mean ± SD (*grey: r-FX, blue: FX-F174A, orange: FX-F174S*). Ab indicates antibody; anti-K1, anti-K2, and anti-K1, K2, C indicate TFPI blocking antibodies against: Kunitz 1 domain; the Kunitz 2 domain; or the Kunitz 1 domain, Kunitz 2 domain and C-terminus, respectively. Thrombin formation was triggered by the addition of 1 pM TF in the presence of 20 µM PCPS and initiated with $CaCl_2$ and a thrombin fluorogenic substrate as detailed in 'Materials and Methods'. *p<0.05, **p<0.01, ***p<0.001, ****p<0.0001 according to one-way ANOVA. The statistically significant differences given are compared to the respective data in the absence of antibodies (no ab). Data sets are representatives of two to three independent experiments.

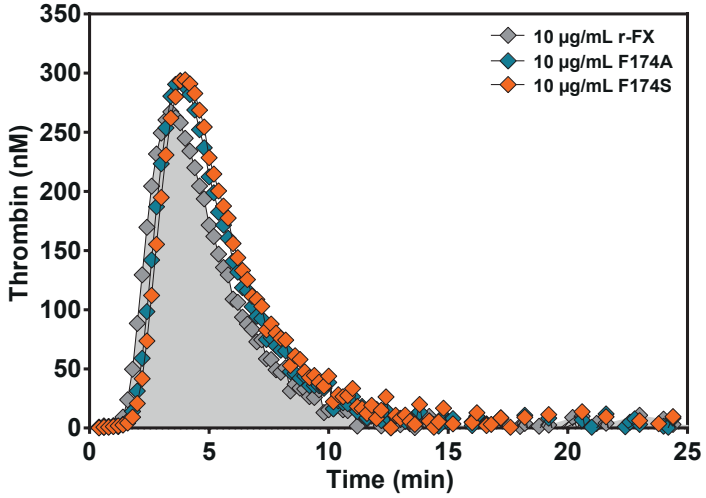

Supplementary figure 5. Thrombin generation in the absence of direct factor Xa inhibitors. Thrombin generation was measured for 30 min at 37°C in FX-deficient plasma supplemented with 10 µg/mL of r-FX (*grey diamonds; area under the curve*), FX-F174A (*blue diamonds)* or FX-F174S (*orange diamonds*). Thrombin formation was triggered by the addition of 6 pM TF in the presence of 20 µM PCPS and initiated with $CaCl_2$ and a thrombin fluorogenic substrate as detailed in 'Materials and Methods'.

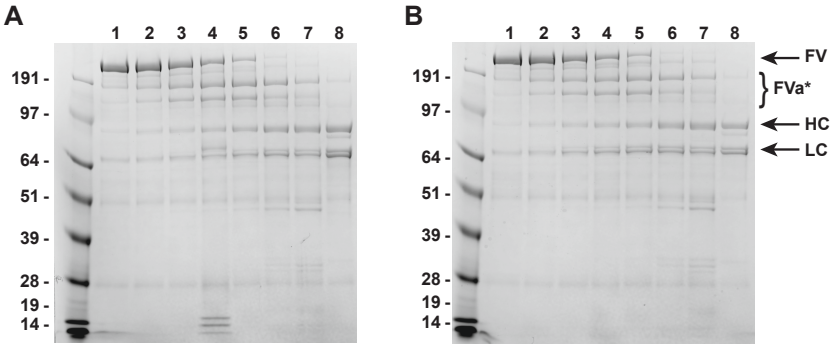

Supplementary figure 6. SDS-PAGE analysis of factor V activation by F174-substituted factor Xa variants. Plasma derived (pd)-FV (455 nM) was incubated for 10min at 25°C with increasing concentrations (0 – 100 nM) of **(A)** recombinant factor Xa (r-FXa) or **(B)** FXa-F174A in the presence of 50 µM PCPS. Samples (3 µg/lane) were subjected to SDS-PAGE under reducing conditions using the MOPS buffer system and visualized by staining with Coomassie Brilliant Blue. Lanes 1-7: pd-FV incubated with 0, 1, 5, 10, 20, 50, or 100 nM FXa; lane 8: thrombin-activated pd-FV (25 nM thrombin, 15min at 37°C). The protein bands corresponding to single chain uncleaved pd-FV (FV), partially activated FV (FVa*), FVa heavy chain (HC), FVa light chain (LC), and the apparent molecular weights of the standards (kDa) are indicated. The data represents a single experiment.

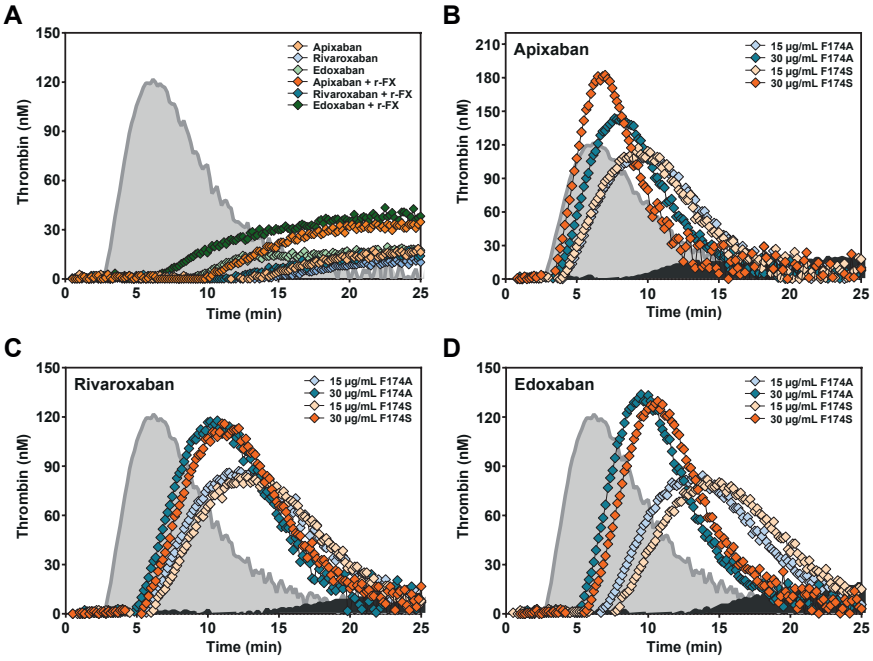

Supplementary figure 7. Correction of thrombin generation at a limited tissue factor concentration in the presence of the direct factor Xa inhibitors. Thrombin generation was measured for 60 min at 37°C in normal pooled plasma (NPP) supplemented with **(A)** 1 µM apixaban, rivaroxaban, or edoxaban in the absence (*yellow, light blue, or light green diamonds, respectively*) or with addition of 60 µg/mL r-FX (orange, dark blue or dark green, respectively), or **(B-D)** 15-30 µg/mL FX-F174A (*light blue-dark blue diamonds*) or FX-F174S (*yellow-orange diamonds*) and 1 µM apixaban **(B)**, rivaroxaban **(C)** or edoxaban **(D)**. Thrombin formation was triggered by the addition of 2 pM TF in the presence of 20 µM PCPS and initiated with $CaCl_2$ and a thrombin fluorogenic substrate as detailed in 'Materials and Methods'. The thrombin generation curves of NPP in the absence **(A-D)** (light gray area under the curve) or presence **(B-D)** (dark gray area under the curve) of the inhibitors are shown. Data sets are representatives of three independent experiments.

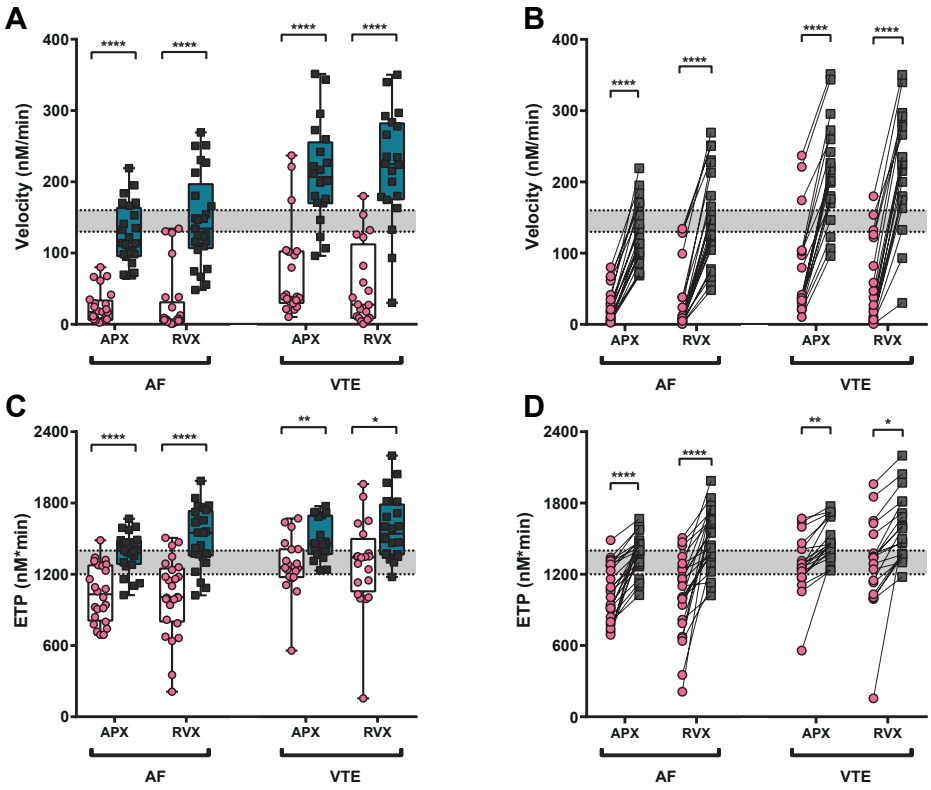

Supplementary figure 8. Velocity of thrombin generation and endogenous thrombin potential (ETP) in atrial fibrillation and venous thromboembolism patient plasma. Thrombin generation was measured for 60 min at 37°C in plasma from atrial fibrillation (AF) or venous thromboembolism (VTE) patients treated with either apixaban (APX) or rivaroxaban (RVX) in the absence (*pink dots*) or supplemented (*grey squares*) with 30 µg/mL FX-F174A. Thrombin formation was triggered by the addition of 6 pM TF in the presence of 20 µM PCPS and initiated with CaCl2 and a thrombin fluorogenic substrate as detailed in 'Materials and Methods'. The thrombin generation velocity **(A-B)** and ETP **(C-D)** are shown. Thrombin generation values of the individual patient plasma in the absence or supplemented with FX-F174A are shown by connected lines **(B, D)**. Bars represent the mean, grey dotted area represents NPP values (n=13; velocity, 130-160 nM/min; ETP, 1200-1400 nM*min). *p<0.05, **p<0.01, ***p<0.001, ****p<0.0001 according to one-way ANOVA. Each data point represents a single measurement performed for each patient sample.

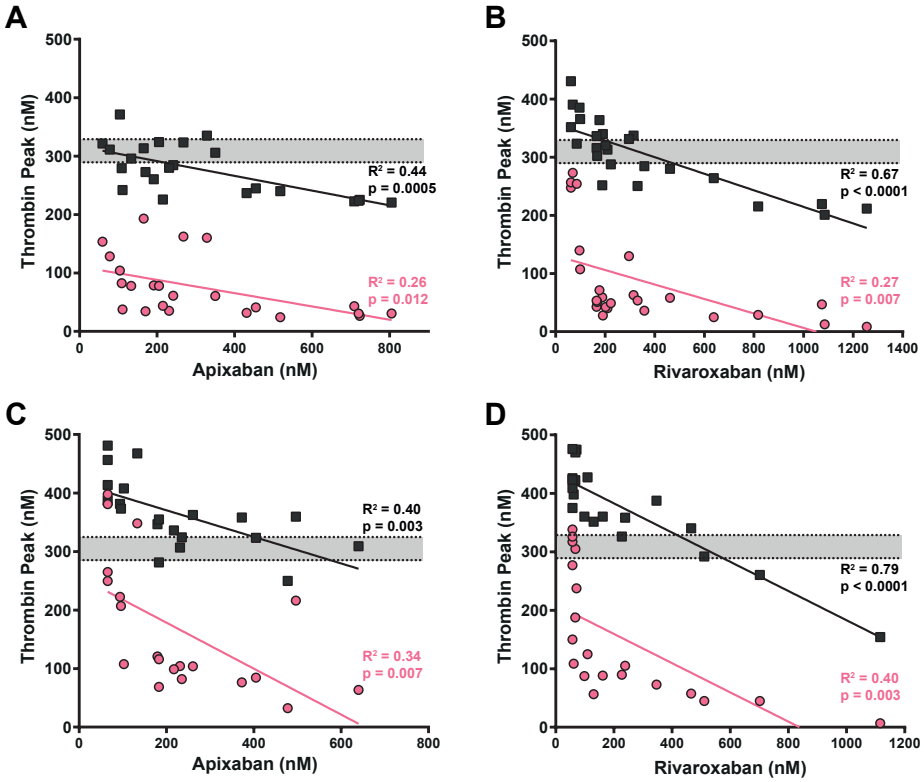

Supplementary figure 9. Correlation between the thrombin peak height and factor Xa inhibitor plasma concentration in patients plasma. Thrombin generation was measured for 60 min at 37°C in plasma from atrial fibrillation **(A-B)** or venous thromboembolism **(C-D)** patients treated with either apixaban or rivaroxaban in the absence (*pink dots*) or presence (*grey squares*) of 30 µg/mL FX-F174A. Thrombin formation was triggered by the addition of 6 pM TF in the presence of 20 µM PCPS and initiated with $CaCl_2$ and a thrombin fluorogenic substrate as detailed in 'Materials and Methods'. The thrombin peak height is presented and lines represent the correlation drawn by fitting the data to a linear regression function upon which the coefficient of determination (R^2) and p-values of the linear regression were obtained; grey dotted area represents NPP values (n=13; thrombin peak, 290-330 nM). Each data point represents a single measurement performed for each patient sample.

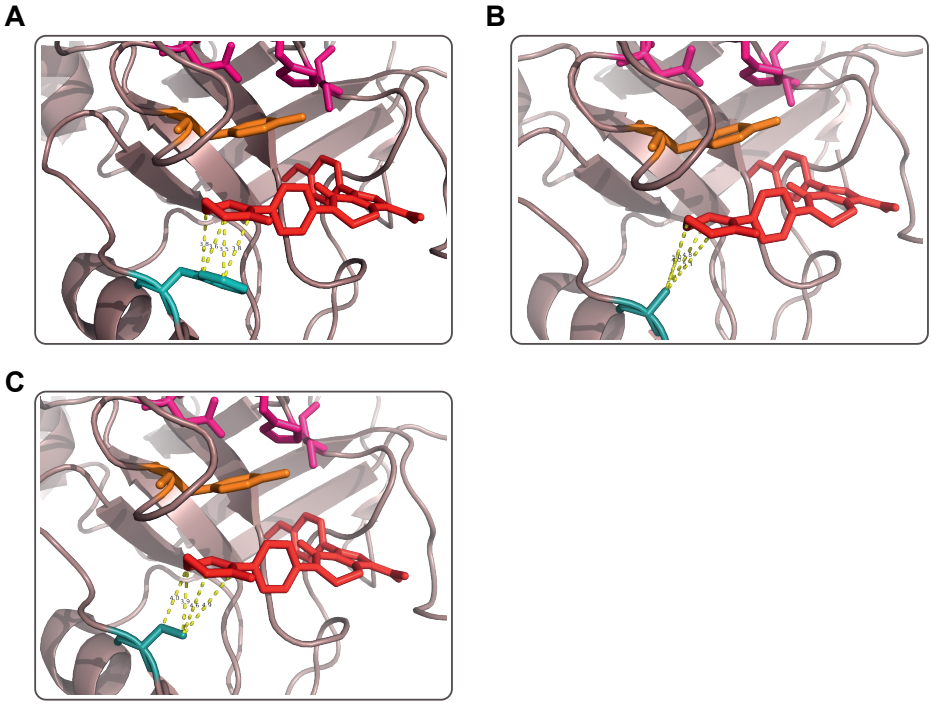

Supplementary Figure 10. Phenylalanine 174 substitution in the factor Xa S4 subsite. (A) X-ray structure of apixaban bound to wild-type factor Xa (FXa; PDB 2P16)[5] shown in line configuration and the modelled structure of phenylalanine 174 substitution with alanine **(B;** FXa-F174A**)** or serine **(C;** FXa-F174S**)**. Interatomic distances between residue 174 and the P_4 moiety of apixaban are indicated by yellow dashed lines (wild-type FXa (3.5-3.8 Å), FXa-F174A (4.0-5.3 Å), FXa-F174S (3.9-4.9 Å)). Apixaban is shown in red. Tyrosine 99 (*orange stick*), residue 174 (*teal stick*) and the catalytic triad residues (His^{57}, Asp^{102}, and Ser^{195}; *magenta sticks*) are indicated. The figure was created using PyMol.

	Apixaban[a] IC_{50} (nM)	Rivaroxaban[a] IC_{50} (nM)	Edoxaban[a] IC_{50} (nM)	Apixaban[b] IC_{50} (nM)	Rivaroxaban[b] IC_{50} (nM)	Edoxaban[b] IC_{50} (nM)
r-FX	121 ± 31	204 ± 28	118 ± 24	166 ± 16	30 ± 4	60 ± 9
FX-F174A	1813 ± 184	3477 ± 583	1243 ± 222	1813 ± 229	1175 ± 439	712 ± 109
FX-F174S	4238 ± 965	3200 ± 405	1385 ± 262	4074 ± 661	1276 ± 98	711 ± 84

Supplementary Table 1. Half maximal inhibitory concentration (IC_{50}) of factor X variants in thrombin generation. IC_{50} values determined using thrombin generation in the presence of 6 pM[a] or 2 pM[b] tissue factor were obtained as described in 'Materials and Methods'. Fitted values ± 1 standard deviation of the induced fit are representative of three independent experiments.

	Intrinsic tenase K_M (μM)	Intrinsic tenase k_{cat} (min^{-1})	Extrinsic tenase K_M (μM)	Extrinsic tenase k_{cat} (min^{-1})
r-FX	275 ± 50	27.5 ± 1.6	502 ± 55	32.5 ± 1.3
FX-F174A	308 ± 51	27.3 ± 1.5	349 ± 54	32.7 ± 1.4
FX-F174S	345 ± 36	24.6 ± 0.9	320 ± 36	31.0 ± 1.1

Supplementary table 2. Kinetic parameters of factor X activation. The kinetic constants for the activation of the factor X variants by either the intrinsic or extrinsic tenase complexes were obtained as described in 'Materials and Methods'. Fitted values ± 1 standard deviation of the induced fit are representative of two to three independent experiments.

References

1 Wendelboe, A. M. & Raskob, G. E. Global Burden of Thrombosis: Epidemiologic Aspects. *Circ Res* **118**, 1340-1347, doi:10.1161/CIRCRESAHA.115.306841 (2016).

2 Zhang, P. *et al.* Discovery of betrixaban (PRT054021), N-(5-chloropyridin-2-yl)-2-(4-(N,N-dimethylcarbamimidoyl)benzamido)-5-methoxybenz amide, a highly potent, selective, and orally efficacious factor Xa inhibitor. *Bioorg Med Chem Lett* **19**, 2179-2185, doi:10.1016/j.bmcl.2009.02.111 (2009).

3 Furugohri, T. *et al.* DU-176b, a potent and orally active factor Xa inhibitor: in vitro and in vivo pharmacological profiles. *J Thromb Haemost* **6**, 1542-1549, doi:10.1111/j.1538-7836.2008.03064.x (2008).

4 Roehrig, S. *et al.* Discovery of the novel antithrombotic agent 5-chloro-N-({(5S)-2-oxo-3-[4-(3-oxomorpholin-4-yl)phenyl]-1,3-oxazolidin-5-yl}methyl)thiophene- 2-carboxamide (BAY 59-7939): an oral, direct factor Xa inhibitor. *J Med Chem* **48**, 5900-5908, doi:10.1021/jm050101d (2005).

5 Pinto, D. J. *et al.* Discovery of 1-(4-methoxyphenyl)-7-oxo-6-(4-(2-oxopiperidin-1-yl)phenyl)-4,5,6,7-tetrahydro-1H -pyrazolo[3,4-c]pyridine-3-carboxamide (apixaban, BMS-562247), a highly potent, selective, efficacious, and orally bioavailable inhibitor of blood coagulation factor Xa. *J Med Chem* **50**, 5339-5356, doi:10.1021/jm070245n (2007).

6 Hauel, N. H. *et al.* Structure-based design of novel potent nonpeptide thrombin inhibitors. *J Med Chem* **45**, 1757-1766, doi:10.1021/jm0109513 (2002).

7 Weitz, J. I. & Harenberg, J. New developments in anticoagulants: Past, present and future. *Thrombosis and haemostasis* **117**, 1283-1288, doi:10.1160/TH16-10-0807 (2017).

8 Connolly, S. J. *et al.* Dabigatran versus warfarin in patients with atrial fibrillation. *N Engl J Med* **361**, 1139-1151, doi:10.1056/NEJMoa0905561 (2009).

9 Patel, M. R. *et al.* Rivaroxaban versus warfarin in nonvalvular atrial fibrillation. *N Engl J Med* **365**, 883-891, doi:10.1056/NEJMoa1009638 (2011).

10 Agnelli, G. *et al.* Oral apixaban for the treatment of acute venous thromboembolism. *N Engl J Med* **369**, 799-808, doi:10.1056/NEJMoa1302507 (2013).

11 Deitelzweig, S. B., Johnson, B. H., Lin, J. & Schulman, K. L. Prevalence of clinical venous thromboembolism in the USA: current trends and future projections. *Am J Hematol* **86**, 217-220, doi:10.1002/ajh.21917 (2011).

12 Chugh, S. S. *et al.* Worldwide epidemiology of atrial fibrillation: a Global Burden of Disease 2010 Study. *Circulation* **129**, 837-847, doi:10.1161/CIRCULATIONAHA.113.005119 (2014).

13 Nazha, B. *et al.* Periprocedural Outcomes of Direct Oral Anticoagulants Versus Warfarin in Nonvalvular Atrial Fibrillation. *Circulation* **138**, 1402-1411, doi:10.1161/CIRCULATIONAHA.117.031457 (2018).

14 Sharma, M., Cornelius, V. R., Patel, J. P., Davies, J. G. & Molokhia, M. Efficacy and Harms of Direct Oral Anticoagulants in the Elderly for Stroke Prevention in Atrial Fibrillation and Secondary Prevention of Venous Thromboembolism: Systematic Review and Meta-Analysis. *Circulation* **132**, 194-204, doi:10.1161/CIRCULATIONAHA.114.013267 (2015).

15 Loo, S. Y., Dell'Aniello, S., Huiart, L. & Renoux, C. Trends in the prescription of novel oral anticoagulants in UK primary care. *Br J Clin Pharmacol* **83**, 2096-2106, doi:10.1111/bcp.13299 (2017).

16 Zhu, J., Alexander, G. C., Nazarian, S., Segal, J. B. & Wu, A. W. Trends and Variation in Oral Anticoagulant Choice in Patients with Atrial Fibrillation, 2010-2017. *Pharmacotherapy* **38**, 907-920, doi:10.1002/phar.2158 (2018).

17 Connolly, S. J. *et al.* Full Study Report of Andexanet Alfa for Bleeding Associated with Factor Xa Inhibitors. *N Engl J Med* **380**, 1326-1335, doi:10.1056/NEJMoa1814051 (2019).

18 January, C. T. *et al.* 2019 AHA/ACC/HRS Focused Update of the 2014 AHA/ACC/HRS Guideline for the Management of Patients With Atrial Fibrillation: A Report of the American College of Cardiology/American Heart Association Task Force on Clinical Practice Guidelines and the Heart Rhythm Society in Collaboration With the Society of Thoracic Surgeons. *Circulation* **140**, e125-e151, doi:10.1161/CIR.0000000000000665 (2019).
19 Christensen, H. *et al.* European Stroke Organisation Guideline on Reversal of Oral Anticoagulants in Acute Intracerebral Haemorrhage. *Eur Stroke J* **4**, 294-306, doi:10.1177/2396987319849763 (2019).
20 Lip, G. Y. H. *et al.* Antithrombotic Therapy for Atrial Fibrillation: CHEST Guideline and Expert Panel Report. *Chest* **154**, 1121-1201, doi:10.1016/j.chest.2018.07.040 (2018).
21 Kessler, C. M. & Goldstein, J. N. A New Strategy for Uncontrollable Bleeding After Treatment With Rivaroxaban or Apixaban. *Clinical Advances in Hematology & Oncology* **17**, 1-17 (2019).
22 Schreuder, M., Reitsma, P. H. & Bos, M. H. A. Reversal Agents for the Direct Factor Xa Inhibitors: Biochemical Mechanisms of Current and Newly Emerging Therapies. *Semin Thromb Hemost*, doi:10.1055/s-0040-1709134 (2020).
23 Bos, M. H. A., Van 't Veer, C. & Reitsma, P. H. Molecular biology and biochemistry of the coagulation factors and pathways of hemostasis. *Williams Hematology* **9th edn.**, 1915–1948 (2016).
24 Lu, G. *et al.* A specific antidote for reversal of anticoagulation by direct and indirect inhibitors of coagulation factor Xa. *Nat Med* **19**, 446-451, doi:10.1038/nm.3102 (2013).
25 Marlu, R. & Polack, B. Gla-domainless factor Xa: molecular bait to bypass a blocked tenase complex. *Haematologica* **97**, 1165-1172, doi:10.3324/haematol.2011.055699 (2012).
26 Ersayin, A. *et al.* Catalytically inactive Gla-domainless factor Xa binds to TFPI and restores ex vivo coagulation in hemophilia plasma. *Haematologica* **102**, e483-e485, doi:10.3324/haematol.2017.174037 (2017).
27 Schreuder, M., Reitsma, P. H. & Bos, M. H. A. Blood coagulation factor Va's key interactive residues and regions for prothrombinase assembly and prothrombin binding. *J Thromb Haemost* **17**, 1229-1239, doi:10.1111/jth.14487 (2019).
28 Huntington, J. A., Read, R. J. & Carrell, R. W. Structure of a serpin-protease complex shows inhibition by deformation. *Nature* **407**, 923-926, doi:10.1038/35038119 (2000).
29 Jourdi, G. *et al.* FXa-alpha2-Macroglobulin Complex Neutralizes Direct Oral Anticoagulants Targeting FXa In Vitro and In Vivo. *Thrombosis and haemostasis* **118**, 1535-1544, doi:10.1055/s-0038-1667014 (2018).
30 Thalji, N. K. *et al.* A rapid pro-hemostatic approach to overcome direct oral anticoagulants. *Nat Med* **22**, 924-932, doi:10.1038/nm.4149 (2016).
31 Toso, R., Zhu, H. & Camire, R. M. The conformational switch from the factor X zymogen to protease state mediates exosite expression and prothrombinase assembly. *J Biol Chem* **283**, 18627-18635, doi:10.1074/jbc.M802205200 (2008).
32 Verhoef, D. *et al.* Engineered factor Xa variants retain procoagulant activity independent of direct factor Xa inhibitors. *Nat Commun* **8**, 528, doi:10.1038/s41467-017-00647-9 (2017).
33 Higgins, D. L. & Mann, K. G. The interaction of bovine factor V and factor V-derived peptides with phospholipid vesicles. *J Biol Chem* **258**, 6503-6508 (1983).
34 Toso, R. & Camire, R. M. Removal of B-domain sequences from factor V rather than specific proteolysis underlies the mechanism by which cofactor function is realized. *J Biol Chem* **279**, 21643-21650, doi:10.1074/jbc.M402107200 (2004).
35 Camire, R. M., Larson, P. J., Stafford, D. W. & High, K. A. Enhanced gamma-carboxylation of recombinant factor X using a chimeric construct containing the prothrombin propeptide. *Biochemistry* **39**, 14322-14329, doi:10.1021/bi001074q (2000).

36 Krishnaswamy, S. & Walker, R. K. Contribution of the prothrombin fragment 2 domain to the function of factor Va in the prothrombinase complex. *Biochemistry* **36**, 3319-3330, doi:10.1021/bi9623993 (1997).
37 Bos, M. H. *et al.* Venom factor V from the common brown snake escapes hemostatic regulation through procoagulant adaptations. *Blood* **114**, 686-692, doi:10.1182/blood-2009-02-202663 (2009).
38 Peraramelli, S. *et al.* Role of exosite binding modulators in the inhibition of Fxa by TFPI. *Thrombosis and haemostasis* **115**, 580-590, doi:10.1160/TH15-04-0354 (2016).
39 Abraham, M. J. *et al.* GROMACS: High performance molecular simulations through multi-level parallelism from laptops to supercomputers. *SoftwareX* **1-2**, 19-25 (2015).
40 Lu, G., Broze, G. J., Jr. & Krishnaswamy, S. Formation of factors IXa and Xa by the extrinsic pathway: differential regulation by tissue factor pathway inhibitor and antithrombin III. *J Biol Chem* **279**, 17241-17249, doi:10.1074/jbc.M312827200 (2004).
41 Zur, M. & Nemerson, Y. Kinetics of factor IX activation via the extrinsic pathway. Dependence of Km on tissue factor. *J Biol Chem* **255**, 5703-5707 (1980).
42 Renatus, M. *et al.* Structural mapping of the active site specificity determinants of human tissue-type plasminogen activator. Implications for the design of low molecular weight substrates and inhibitors. *J Biol Chem* **272**, 21713-21719, doi:10.1074/jbc.272.35.21713 (1997).
43 Olson, S. T. *et al.* Accelerating ability of synthetic oligosaccharides on antithrombin inhibition of proteinases of the clotting and fibrinolytic systems. Comparison with heparin and low-molecular-weight heparin. *Thrombosis and haemostasis* **92**, 929-939, doi:10.1160/TH04-06-0384 (2004).
44 Camire, R. M. Prothrombinase assembly and S1 site occupation restore the catalytic activity of FXa impaired by mutation at the sodium-binding site. *J Biol Chem* **277**, 37863-37870, doi:10.1074/jbc.M203692200 (2002).
45 Li, W., Johnson, D. J., Esmon, C. T. & Huntington, J. A. Structure of the antithrombin-thrombin-heparin ternary complex reveals the antithrombotic mechanism of heparin. *Nat Struct Mol Biol* **11**, 857-862, doi:10.1038/nsmb811 (2004).
46 Johnson, D. J., Li, W., Adams, T. E. & Huntington, J. A. Antithrombin-S195A factor Xa-heparin structure reveals the allosteric mechanism of antithrombin activation. *EMBO J* **25**, 2029-2037, doi:10.1038/sj.emboj.7601089 (2006).
47 Parasrampuria, D. A. & Truitt, K. E. Pharmacokinetics and Pharmacodynamics of Edoxaban, a Non-Vitamin K Antagonist Oral Anticoagulant that Inhibits Clotting Factor Xa. *Clin Pharmacokinet* **55**, 641-655, doi:10.1007/s40262-015-0342-7 (2016).
48 Mueck, W., Stampfuss, J., Kubitza, D. & Becka, M. Clinical pharmacokinetic and pharmacodynamic profile of rivaroxaban. *Clin Pharmacokinet* **53**, 1-16, doi:10.1007/s40262-013-0100-7 (2014).
49 Byon, W., Garonzik, S., Boyd, R. A. & Frost, C. E. Apixaban: A Clinical Pharmacokinetic and Pharmacodynamic Review. *Clin Pharmacokinet* **58**, 1265-1279, doi:10.1007/s40262-019-00775-z (2019).
50 van Veen, J. J., Gatt, A. & Makris, M. Thrombin generation testing in routine clinical practice: are we there yet? *Br J Haematol* **142**, 889-903, doi:10.1111/j.1365-2141.2008.07267.x (2008).
51 Hertzberg, M. Biochemistry of factor X. *Blood Rev* **8**, 56-62, doi:10.1016/0268-960x(94)90007-8 (1994).
52 Schuijt, T. J. *et al.* Factor Xa activation of factor V is of paramount importance in initiating the coagulation system: lessons from a tick salivary protein. *Circulation* **128**, 254-266, doi:10.1161/CIRCULATIONAHA.113.003191 (2013).
53 Shapiro, A. D. *et al.* Subcutaneous concizumab prophylaxis in hemophilia A and hemophilia A/B with inhibitors: Phase 2 trial results. *Blood*, doi:10.1182/blood.2019001542 (2019).

54 Hilden, I. *et al.* Hemostatic effect of a monoclonal antibody mAb 2021 blocking the interaction between FXa and TFPI in a rabbit hemophilia model. *Blood* **119**, 5871-5878, doi:10.1182/blood-2012-01-401620 (2012).
55 Waters, E. K., Sigh, J., Friedrich, U., Hilden, I. & Sorensen, B. B. Concizumab, an anti-tissue factor pathway inhibitor antibody, induces increased thrombin generation in plasma from haemophilia patients and healthy subjects measured by the thrombin generation assay. *Haemophilia* **23**, 769-776, doi:10.1111/hae.13260 (2017).
56 Broze, G. J., Jr. & Girard, T. J. Tissue factor pathway inhibitor: structure-function. *Front Biosci (Landmark Ed)* **17**, 262-280, doi:10.2741/3926 (2012).
57 Wood, J. P., Ellery, P. E., Maroney, S. A. & Mast, A. E. Biology of tissue factor pathway inhibitor. *Blood* **123**, 2934-2943, doi:10.1182/blood-2013-11-512764 (2014).
58 Qu, S. Y. *et al.* An unexpected dynamic binding mode between coagulation factor X and Rivaroxaban reveals importance of flexibility in drug binding. *Chem Biol Drug Des* **94**, 1664-1671, doi:10.1111/cbdd.13568 (2019).
59 Krishnaswamy, S. Exosite-driven substrate specificity and function in coagulation. *J Thromb Haemost* **3**, 54-67, doi:10.1111/j.1538-7836.2004.01021.x (2005).
60 Schreuder, M. *et al.* Evolutionary adaptations in Pseudonaja textilis venom factor X induce zymogen activity and resistance to the intrinsic tenase complex. *Accepted in Thrombosis and Haemostasis* (2020).
61 Siegal, D. M. *et al.* Andexanet Alfa for the Reversal of Factor Xa Inhibitor Activity. *N Engl J Med* **373**, 2413-2424, doi:10.1056/NEJMoa1510991 (2015).
62 Menegatti, M. & Peyvandi, F. Factor X deficiency. *Semin Thromb Hemost* **35**, 407-415, doi:10.1055/s-0029-1225763 (2009).
63 Pryzdial, E. L. & Kessler, G. E. Kinetics of blood coagulation factor Xaalpha autoproteolytic conversion to factor Xabeta. Effect on inhibition by antithrombin, prothrombinase assembly, and enzyme activity. *J Biol Chem* **271**, 16621-16626, doi:10.1074/jbc.271.28.16621 (1996).